Journal of Renewable Energy and Sustainable Development (RESD) Volume 2, Issue 2, December 2016 - ISSN 2356-8569
http://dx.doi.org/10.21622/RESD.2016.02.2.096

Three-to-Five-Phase Matrix Converter Using Carrier-based PWM Technique

S. M. Allam, Sherif M. Dabour and Essam M. Rashad
Department of Electrical Power and Machines Engineering, Tanta University, Tanta, Egypt
sm_allam@yahoo.com, shdabour@yahoo.com,
emrashad@ieee.org

Abstract - This paper proposes a simple carrier-based PWM (CBPWM) technique to control the three-to five-phase Direct Matrix Converter (3×5 DMC). The proposed technique uses the indirect modulation approach to control the 3×5 DMC such as a three-phase bidirectional rectifier followed by five-phase voltage source inverter (VSI). Based on this approach, it is possible to synthesize the desired five-phase output voltages with sinusoidal three-phase input currents and unity input power factor. A CBPWM method is suggested for each stage independently including both linear and overmodulation operating modes. By the proposed technique, in both operating modes, the maximum possible overall Voltage Transfer Ratio (VTR) is achieved. Moreover, this technique allows the input power factor to be controlled by controlling the input current displacement angle. The feasibility of the proposed technique has been verified by a series of simulation and experimental results based on Matlab/Simulink and dSPACE-DS1104 platform. The results show that a sinusoidal output and input waveforms can be achieved with a maximum possible VTR in the linear region. However, in the overmodulation region, a maximum possible VTR is achieved at the cost of some distortion of output and input waveforms. Therefore, this technique can be used for the application where a higher VTR is essential.

Keywords - Five-phase, matrix converter, carrier-based PWM, overmodulation.

I. INTRODUCTION

N recent years, Matrix Converter (MC) is attracting extensive attention as a direct power converter that can convert the electrical energy from an ac source to an ac load [1]-[3]. The MC uses a matrix of semiconductor devices to connect the m-phase supply to the n-phase load directly [2]. It has been recognized as an alternative approach to overcome the drawbacks of conventional VSIs [4]. It also offers some distinct advantages such as: (i) sinusoidal input current and output voltage waveforms, (ii) natural four-quadrant operation, (iii) potential for compact design, and (iv) the input power factor can be fully controlled [4]-[6]. However, reduced output voltage, increased the semiconductor switches, complexity of the modulation technique and sensitivity to supply voltage disturbances are the main drawbacks [7]. Therefore, the industrial applications of this type of converter are limited [1].

Generally, the matrix converter can be represented as a single-stage (direct) or a double-stage (indirect) configuration [3], [7]. The different modulation techniques that can be applied on this type of converter are classified, according to the converter configuration, into two main categories, namely; direct and indirect modulation techniques [8]. The direct modulation technique is based on representing the matrix converter as a single-stage (direct) configuration. In this approach, the output voltage is obtained directly by the product of the input voltage and the switching-states modulation matrix representing the converter. On the other hand, the indirect modulation technique is based on the indirect (double-stage) configuration of the matrix converter in which the converter is represented as a rectifier-inverter combination without any dc-link. Using either direct or indirect configuration of MC, the CBPWM or SVM techniques can be applied.

The matrix converter was firstly introduced as a direct 3×3 phase configuration in [2] and steadily grew, pushed by the progress of the power electronics technology. Firstly, Venturini proposes a direct modulation CBPWM technique for the 3×3 MC [9]. The maximum obtainable output voltage using this technique does not exceed 0.5 of the input supply voltage. However, it has been increased to 0.866 using a third-harmonic injection [10]. On the other hand, the Space Vector Modulation (SVM) technique is found to be a very powerful solution to control the MCs [5]. According to the converter configurations, the SVM technique for controlling the matrix

converters can be classified into direct SVM (DSVM) and indirect SVM (ISVM). The ISVM is proposed for 3×3 MC in [4]-[5]. In addition, the DSVM technique of 3×3 MC is presented in [11]-[12]. Recently, some research works have concentrated on the development of multiphase MC as an alternative to the conventional ac–dc–ac multiphase VSI [8], [13]-[24]. The SVM technique is developed to control the 3×5 MC in the linear modulation operating mode based on DSVM and ISVM [13]-[15]. The maximum obtainable output voltage, based on this modulation technique, equals 0.7887 from the input supply voltage. However, the complexity of the system is increased. In order to reduce the complexity of the multiphase MC system, the CBPWM techniques and Direct/Indirect Duty Cycle techniques have been introduced and developed.

The CBPWM is a simple PWM approach for controlling the MCs, in which the converter switching signals are obtained by comparing the reference modulating signals with a triangular carrier-wave. This technique was firstly reported by [25] for controlling the 3×3 MC, based on the direct converter configuration, in the linear modulation operating mode. A comprehensive solution to extend the operation of this technique in over-modulation operating mode is presented in [26]. This modulation technique has been developed to 3×5, 3×6, 3×7 and 3×9 MCs in [17], [18], [20] and [8] respectively. A new CBPWM technique, based on the indirect converter configuration, is proposed for the 3×3 MC [7]. In addition, a generalized CBPWM method, based on the correlation between SVPWM and CBPWM techniques, is proposed for 3×3 and 3×5 MC [6], [16]. In this method of modulation, one symmetrical triangular-carrier signal is used to generate the gating signals for both rectifier and inverter stages of the IMC. Furthermore, a generalized direct duty ratio based PWM technique has been presented to control the 3×k MC [21]. A specific case of the 3×5 MC is chosen to illustrate the control algorithm proposed in [21]. However, in the previous works [13]-[17] and [21], it is found that the output phase-voltage of the 3×5 MC is limited to 78.87 percent of the input phase-voltage. This value represents the theoretical limit of the output voltage in the linear operating mode. The output voltage can be increased if the converter is operated in the over-modulation mode.

Therefore, this paper aims to present a simple and more efficient CBPWM technique to control three to five-phase matrix converters, which can be used to supply a five-phase induction motor drive system that delivers some advantageous features for industrial applications. The basic concept of the proposed technique is already published in [27]. Thanks to its simplicity, the proposed technique will be based on the indirect modulation of the 3×5 MC which control the converter as a double stage converter. Therefore, the carrier based PWM methods are applied for each stage independently. The proposed modulation will maximize the converter VTR by operating the converter in the overmodulation mode as well as in the linear modulation mode. It also controls the input power factor by controlling the input current displacement angle. The proposed modulation technique is verified using simulation and experimental results based on a laboratory prototype and the dSPACE-DS1104 controller platform and the results are compared by the existing SVM technique.

II. THREE- TO FIVE-PHASE MATRIX CONVERTER TOPOLOGIES

The power circuit topology of three- to five-phase (3×5) MC for the direct and indirect configuration are shown in Fig. 1 and Fig. 2. The direct configuration uses a 3×5 matrix of bidirectional switches as depicted by Fig. 1 to connect any of the input phases (A, B or C) to any of the output phases (a, b, … or e). Therefore, the output voltages (v_a, v_b, … and v_e) can be directly determined from the input three-phase voltages (v_A, v_B and v_C). On the other hand, the indirect configuration uses three-phase bidirectional rectifier and five-phase inverter as shown in Fig. 2.

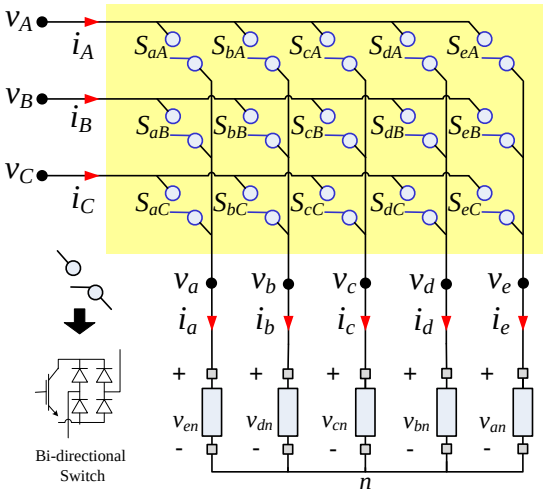

Fig .1. Power circuit topology of the direct configuration of the 3×5 MC.

http://dx.doi.org/10.21622/RESD.2016.02.2.096

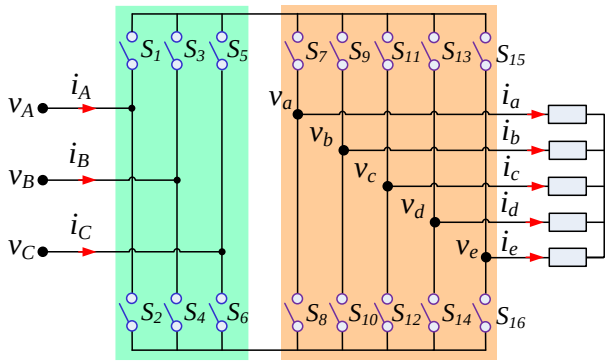

Fig .2. Power circuit topology of the indirect configuration of the 3×5 MC.

III. PROPOSED CBPWM ALGORITHM FOR 3×5 MC

Carrier-based PWM technique has been obtained by comparing the modulation signals with a high frequency carrier-wave. Since the proposed technique is based on the indirect modulation of the MC, it is necessary to determine a set of modulating signals for the rectifier and inverter stages and compare it with the carrier wave to obtain the switching signals. The resultant switching signals from the comparisons are combined to get the overall switching-states modulation matrix of the 3×5 MC. In the proposed technique, due to the nature of the rectifier and inverter operation, the control of the rectifier stage uses a saw-tooth carrier signal, while a symmetrical triangular carrier signal is used for the inverter. In both stages there are three-operating modes; 1) linear mode, 2) overmodulation mode and 3) stepped operating mode. In the following subsections, an illustration of the proposed modulation technique for both stages is introduced.

A. *Modulation of Rectifier stage*

The rectifier stage has to generate a virtual dc-link voltage (V_{dc}) by chopping input three-phase voltages. This operation is performed by the rectifier switches, which are divided into two groups; namely upper $\{S_1,S_3,S_5\}$ and lower $\{S_2,S_4,S_6\}$ groups.

Three switches in a group connect all input phases to one terminal of the dc-link. Therefore, in order to avoid short-circuit on the input phases or open-circuit on the dc-link only one switch in a group must be turned on at a time. This means

$$S_1 + S_3 + S_5 = 1$$
$$S_2 + S_4 + S_6 = 1 \qquad (1)$$

The virtual dc-link voltage can be obtained from the input voltages by the rectifier-switching matrix as follows:

$$\begin{bmatrix} +\frac{1}{2}v_{dc} \\ -\frac{1}{2}v_{dc} \end{bmatrix} = \begin{bmatrix} S_1 & S_3 & S_5 \\ S_2 & S_4 & S_6 \end{bmatrix} . \begin{bmatrix} v_A \\ v_B \\ v_C \end{bmatrix} \qquad (2)$$

Assuming that, the three-phase input voltages are balanced and given by:

$$\begin{bmatrix} v_A \\ v_B \\ v_C \end{bmatrix} = \hat{V}_i \begin{bmatrix} sin\,\theta_A \\ sin\,\theta_B \\ sin\,\theta_C \end{bmatrix} \qquad (3)$$

where $\hat{V}_i$ is the input peak voltage and $\theta_A = \omega_i t$, $\theta_B = \omega_i t - 2\pi/3$, $\theta_C = \omega_i t + 2\pi/3$ are the respective phase angle with an input angular frequency of ω_i.

1. Rectifier-Stage Modulating Signals Calculations

The modulating signals for the rectifier switches, δ_R (δ_1-δ_6, where $\delta_1$represents the modulating signal of the switch S_1 and so on) can be derived as:

$$\begin{aligned} \delta_{1,2} &= \pm m_R\, sin(\theta_A + \emptyset) \\ \delta_{3,4} &= \pm m_R\, sin(\theta_B + \emptyset) \\ \delta_{5,6} &= \pm m_R\, sin(\theta_C + \emptyset) \end{aligned} \qquad (4)$$

where m_R is the rectifier-stage modulation-index and $\emptyset$ is the input-current displacement-angle. In the linear-modulation operating mode, the rectifier-stage modulation-index m_R does not exceed 0.5 [25].

In order to satisfy the constraint in (1), the summation of the modulating signals of the upper-group switches and that of the lower-group switches should equal one in a switching cycle [26]. However, the modulating signals obtained in (4) do not satisfy this condition. Therefore, offset signals must be added to the modulating signals [26]. Firstly, the absolute value of each modulating signal (d_A, d_B, d_C) is added to cancel the negative half-cycle. Hence, the resultant signals have a lower limit that equals zero. However, the summation of the modulating signals does not

equal one all a time. In order to solve this problem, another offset signal ε should be added to the modulating signals. The modified modulating signals are given by:

$$\begin{aligned}\delta_{1,2} &= \pm m_R \sin(\theta_A + \emptyset) + d_A + \varepsilon \\ \delta_{3,4} &= \pm m_R \sin(\theta_B + \emptyset) + d_B + \varepsilon \\ \delta_{5,6} &= \pm m_R \sin(\theta_C + \emptyset) + d_C + \varepsilon\end{aligned} \quad (5)$$

where

$$\begin{aligned}d_A &= |m_R \sin(\theta_A + \emptyset)| \\ d_B &= |m_R \sin(\theta_B + \emptyset)| \\ d_C &= |m_R \sin(\theta_C + \emptyset)|\end{aligned} \quad (6)$$

$$\varepsilon = (1 - (d_A + d_B + d_C))/3 \quad (7)$$

Therefore, aiding with (5), the modulating signals of all rectifier switches in each switching period can be easily determined. Fig. 3 illustrates the determination process of the rectifier upper-switches modulating signals. The modulating signals of the rectifier lower-switches can be determined by the same manner. The resulting rectifier-stage modulating signals waveforms corresponding to the maximum value of the rectifier-stage modulation-index ($m_R = 0.5$) are shown in Fig. 4.

2. Carrier-based Modulator of the Rectifier-Stage

The function of the carrier-based modulator is to compare the modulating signals with a common triangle carrier-wave in order to determine the switching signals. The proposed modulator is simple to implement and needs only the calculation of the rectifier-stage modulating signals, δ_R. Fig. 5 shows the proposed modulator and the generated switching signals of the rectifier upper-switches in which a triangular carrier-signal of an amplitude in the range of [0, 1] and a frequency of "f_{c1}" are compared with the three regular-sampled (i.e. assumed constant in each switching period) modulating signals of the upper switches (δ_1, δ_3, and δ_5). Hence, the switching signal of the upper switches (S_1, S_3, and S_5) are obtained. Similarly, the switching signals of the lower switches (S_2, S_4, and S_6) can be determined.

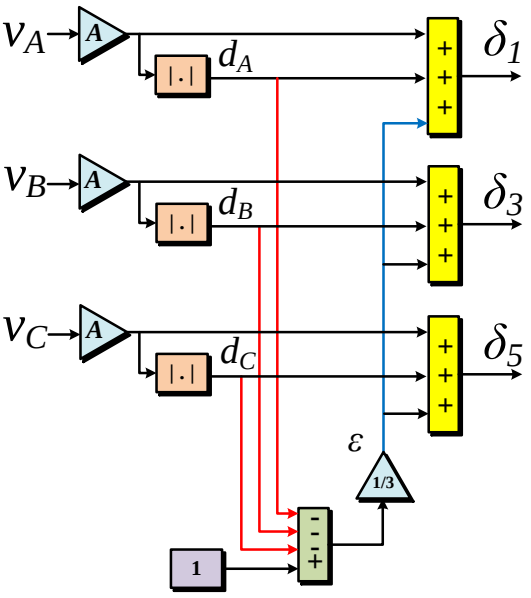

Fig .3. Determination of the rectifier upper-switches modulating-signals, $A = m_R/\hat{V}_i$

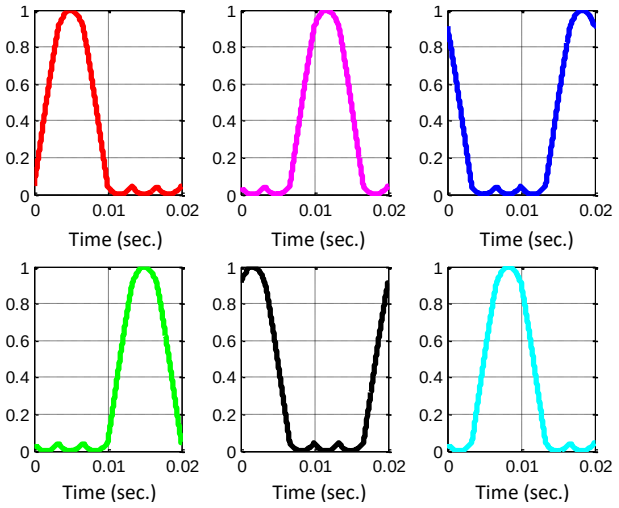

Fig .4. The rectifier stage modulating signals waveforms at $m_R = 0.5$

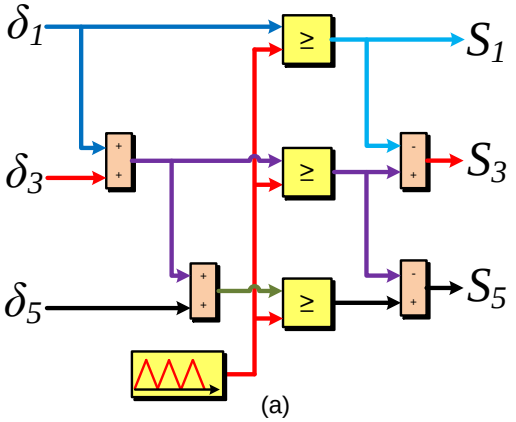

(a)

http://dx.doi.org/10.21622/RESD.2016.02.2.096

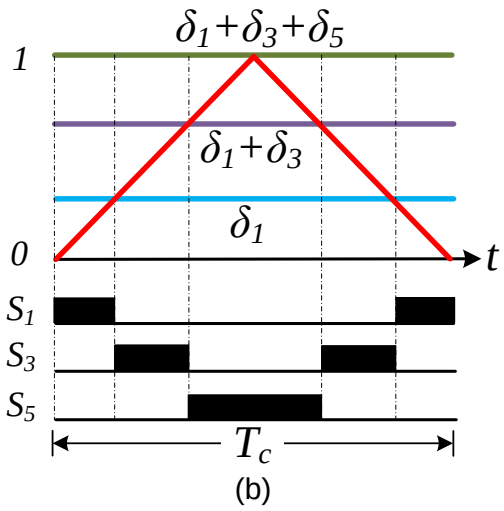

(a) schematic-diagram (b) waveforms

Fig .5. Carrier-based modulator and switching signals for the rectifier upper-switches.

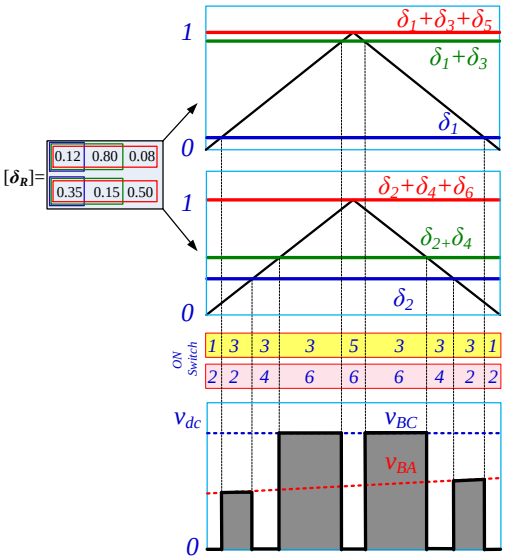

Fig .6. dc-link voltage generation from the rectifier-stage modulator.

3. Generation of the Virtual dc-link Voltage

Once the rectifier switching-signals are determined, the virtual dc-link voltage can be obtained according to (2). Fig. 6 illustrates the process of the instantaneous dc-voltage generation. It is clear to observe that, the dc-voltage level varies between maximum and medium value of the input line-voltage. The average dc-link voltage can be determined by substituting the value of each modulating signal obtained from (4) into the corresponding rectifier switch in (2), this yields;

$$V_{dc} = 3\hat{V}_i m_R \cos \emptyset \qquad (8)$$

Equation (8) shows that the maximum possible dc-link voltage can be obtained at $m_R = 0.5$ and zero input-current displacement angle. Therefore, the maximum possible dc-link voltage in the linear-modulation operating mode is 1.5 times of the peak input phase-voltage. Accordingly, the maximum VTR of the rectifier stage in the linear-modulation operating mode equals 1.5.

4. Rectifier-stage Overmodulation Operating Mode

In order to obtain a maximum allowable dc-link voltage, each switch in the upper group must be turned on when the corresponding input phase voltage is the highest input-voltage at the instant considered [28]. In contrary, each switch in the lower group must be turned on if the corresponding input phase voltage is the lowest input voltage at the instant considered. In other words, in order to obtain the maximum allowable dc-link voltage, the rectifier stage must be operated as a conventional three-phase diode rectifier-circuit. From this concept, the input phase-voltages described in (3) should be divided into six sectors, as shown in Fig. 7, where the polarity of one input phase-voltage is always opposite to the other two phases. This may be defined as a rectifier-stage over-modulation operating mode. An illustration of the proposed over-modulation operating mode, including the switching state of the rectifier switches and the generation of the maximum possible dc-link voltage, is presented in Fig.7. The maximum possible dc-link voltage in this operating mode is 1.654 times of the peak input phase-voltage. Therefore, the maximum obtainable VTR of the rectifier stage in the over-modulation operating mode equals 1.654. Thus, it can be concluded that the proposed rectifier-stage over-modulation mode has the same performance of the corresponding one applied for 3×3 MC [29] and extended for 3×7 MC [20].

In this operating mode of operation, the generation of the rectifier–stage switching signals can be easily implemented according to the flowchart given in Fig.8.

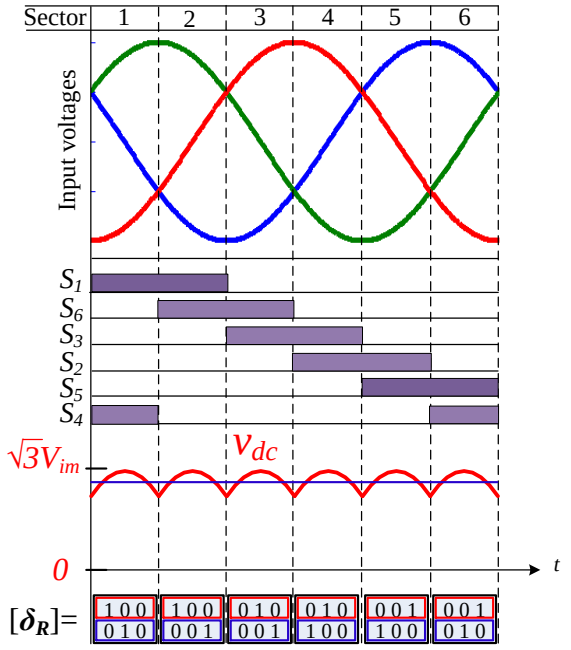

Fig .7. Illusrtation of the rectifer-stage overmodulation operating mode

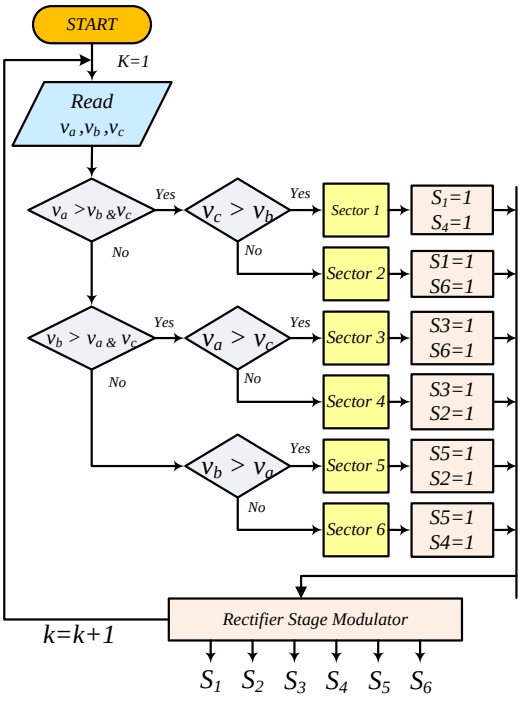

Fig .8. Flowchart showing the generation of the rectifier–stage switching signals in the over-modulation operating mode

B. *Inverter-stage Control (ISC)*

The inverter-stage has to generate the desired output five-phase voltages from the virtual dc-link voltage. This operation is performed aiding with the switching states of the five-phase inverter-switches, which can divided into five groups (legs); namely, leg-*a* {S_7, S_8}, leg-*b* {S_9, S_{10}}, leg-*c* {S_{11}, S_{12}}, leg-*d* {S_{13}, S_{14}} and leg-*e* {S_{15}, S_{16}}.

In order to avoid short-circuit on the virtual dc-link voltage or open-circuit on the load terminals, the two-switches in each leg must be operated in a complementary operating mode. This means;

$$S_j + S_{j+1} = 1 \qquad (9)$$

where j=7, 9, …, 15. The output voltages can be obtained from the dc-link voltage by the inverter switching-matrix as follows:

$$\begin{bmatrix} v_a \\ v_b \\ v_c \\ v_d \\ v_e \end{bmatrix} = \begin{bmatrix} S_7 & S_8 \\ S_9 & S_{10} \\ S_{11} & S_{12} \\ S_{13} & S_{14} \\ S_{15} & S_{16} \end{bmatrix} . \begin{bmatrix} +\frac{1}{2}v_{dc} \\ -\frac{1}{2}v_{dc} \end{bmatrix} \qquad (10)$$

The reference five-phase output voltages are assumed to be balanced and given by:

$$\begin{bmatrix} v_a \\ v_b \\ v_c \\ v_d \\ v_e \end{bmatrix} = \hat{V}_o \begin{bmatrix} sin(\omega_o t) \\ sin(\omega_o t - 2\pi/5) \\ sin(\omega_o t - 4\pi/5) \\ sin(\omega_o t + 4\pi/5) \\ sin(\omega_o t + 2\pi/5) \end{bmatrix} \qquad (11)$$

1. Inverter-stage Modulating Signals Calculations

The modulating signals for the upper switches of inverter stage, δ_I $(\delta_7, \delta_9, \ldots \delta_{15})$ can be obtained according to the general formula used for the five-phase VSI as follows [28];

$$\begin{aligned} \delta_7 &= m_I\, sin(\omega_o t) \\ \delta_9 &= m_I\, sin(\omega_o t - 2\pi/5) \\ \delta_{11} &= m_I\, sin(\omega_o t - 4\pi/5) \\ \delta_{13} &= m_I\, sin(\omega_o t + 4\pi/5) \\ \delta_{15} &= m_I\, sin(\omega_o t + 2\pi/5) \end{aligned} \qquad (12)$$

where δ_7 represents the modulating signal of switch S_7 and so on, m_I is the inverter-stage modulation index and ω_o is the desired output frequency in rad/sec. it is well known that the value of m_I determines the magnitude of the output voltage and it is selected between 0 and 1 for the linear modulation operating mode, while in the overmodulation mode m_I it is greater than one.

http://dx.doi.org/10.21622/RESD.2016.02.2.096

Comparing the modulating signals of (12) with the common carrier signal, results in the appropriate switching signals of the inverter upper-switches. In addition, the switching signals of the inverter lower-switches can be easily obtained as complementary for the corresponding signals of the upper-switches. Due to using pure sinusoidal modulating signals, this modulation technique is generally known as sinusoidal PWM (SPWM) in which the VTR of the inverter stage does not exceed 0.5 in the linear modulation operating mode. However, for optimal utilization of the virtual dc-link voltage, an offset signal should be added to the modulating signals, given in (12). This offset signal is named Injected Zero Sequence Signal (ZSS), δ_{zs} [29]. Different types of the injected zero-sequence signals result in different schemes of CBPWM technique. the Fifth-Harmonic Injection PWM (FHIPWM) and the Continuous Space Vector PWM (CSVPWM) are the widely used schemes [29], [30].

In the FHIPWM scheme, the linear modulation mode of the five-phase inverter stage can be extended by injecting an amount of the fifth order harmonic-signals to the sinusoidal modulating signals. This increases the output voltage without reaching the over-modulation mode limit. The value of δ_{zs} in this scheme is selected as follows [31]:

$$\delta_{zs} = -1/5 m_I sin(\pi/10)\, sin(5\omega_o t) \qquad (13)$$

It is found that this technique can increase the fundamental component of the output voltage up to 5.15% rather than that of SPWM [13].

On the other hand, the value of the injected zero-sequence signal, δ_{zs} in the continuous SVPWM (CSVPWM) scheme is given by [31]-[32]:

$$\delta_{zs} = -1/2(\delta_{MAX} + \delta_{MIN}) \qquad (14)$$

Where

$$\delta_{MAX} = max(\delta_7, \delta_9, \delta_{11}, \delta_{13}, \delta_{15})$$
$$\delta_{MIN} = min(\delta_7, \delta_9, \delta_{11}, \delta_{13}, \delta_{15})$$

The modulating and the injected zero-sequence signals of both FHIPWM and CSVPWM schemes for output frequency of 50Hz are illustrated in Fig. 9. On the other hand, it is well known that the maximum available VTR that can be obtained when the inverter stage is in stepped-wave operation is equal to 0.636 [33].

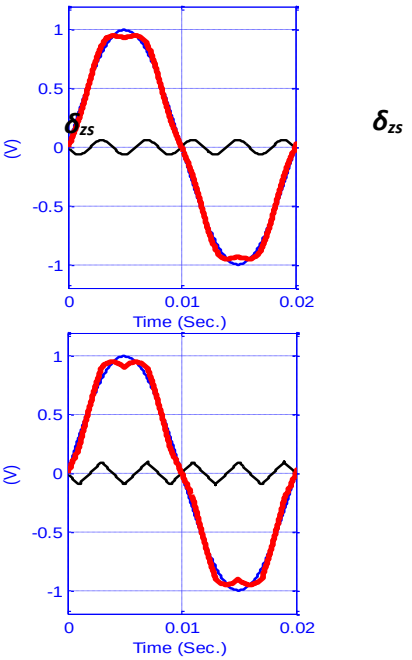

(a) FHIPWM-scheme (b) CSVPWM-scheme

Fig .9. Modulating and injected zero-sequence signals waveforms of both FHIPWM and CSVPWM schemes for output frequency of 50Hz

2. Inverter-stage Carrier-based Modulator

Fig. 10 shows the schematic diagram of the inverter-stage modulator in which the triangular carrier signal of an amplitude in the range of [-1, 1] and a frequency of "f_{c2}" is compared with the five-phase modulating signals of the upper switches. This results in the switching signal of the corresponding switches. By inverting the resulting switching signals, the switching signals of the lower switches can be obtained.

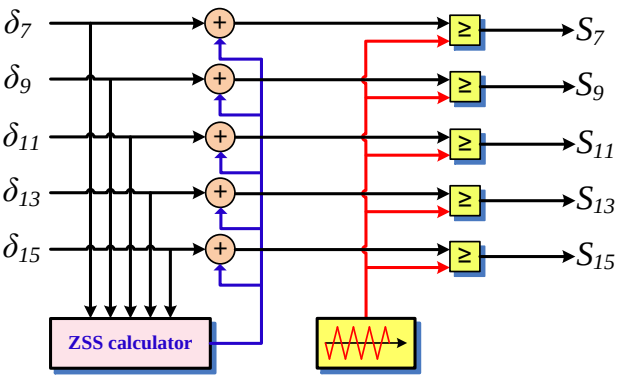

Fig .10. Carrier-based modulator configration of the inverter stage

IV. VOLTAGE TRANSFER RATIO OF 3×5 MC USING THE PROPOSED CBPWM TECHNIQUE

Based on the proposed CBPWM technique of the 3×5 MC, there are two VTRs that should be controlled; the VTR of the inverter-stage, VTR_I and the VTR the rectifier-stage, VTR_R. Hence, the overall VTR can be obtained as:

$$VTR = VTR_R \times VTR_I \qquad (15)$$

Since both stages can be operated in either linear or over-modulation operating modes, the maximum overall VTR in the linear operating mode can be achieved if the VTR of each stage is controlled to be equal to its maximum value in this operating mode. On the other hand, the MC can operate in the over-modulation operating mode if one or both stages are over-modulated. Therefore, the over-modulation operating mode of the MC is classified into three modes; namely, Rectifier-stage over-modulation mode (RSO), Inverter-stage over-modulation mode (ISO) and both stages over-modulation mode (BSO). The overall VTRs of 3×5 MC using the proposed CBPWM technique are given in Table-I.

Table 1. VTRs of 3×5 MC Using the Proposed CBPWM Technique

Rectifier \ Inverter	Linear		ISO (*VTR* = 0.636)
	SPWM (*VTR* = 0.5)	CSVPWM (VTR = 0.525)	
Linear (VTR = 1.5)	0.75	0.7887	0.954
RSO (*VTR* = 1.654)	0.827	0.8697	1.052

It can be observed that the maximum obtainable overall VTR equals 1.052 when both stages are over-modulated. However, when both stages are operated in the linear mode, the maximum overall VTR equals 0.7887. It can be concluded, supported by the proposed modulation technique, that the maximum obtainable overall VTR is exactly the same as that obtained, using the SVM technique, in [14], [15] when both stages are operated in the linear mode. In addition, the VTR can increase when one or both of sides are over-modulated.

V. IMPLEMENTATION PROCEDURE OF THE PROPOSED CBPWM TECHNIQUE TO CONTROL THE 3×5 MC

to control the switches of the 3×5 MC, based on the proposed technique, the switching signals generated by both the rectifier and inverter stages should be firstly combined, based on the presented mathematical model of the converter, using equations (2) and (10). Fig. 11 shows the layout of the implementation procedure of the proposed technique. This procedure is used in both the simulation and experimental processes. Fig. 11 shows that there are two main traces that are used for controlling both the rectifier and inverter stages, including modulating signal and carrier-wave generation, and gating-signals modulators.

It can be clearly observed that the desired rectifier-stage VTR and the input-current displacement angle are defined to calculate the appropriate modulating signals of the rectifier-stage based on (5). From which the rectifier-stage switching signals are obtained via rectifier-stage modulator. On the other hand, the desired inverter-stage VTR and the output frequency are used to determine the modulating signals of the inverter-stage based on (12). Hence, the switching signals of the inverter-stage can be generated via inverter-stage modulator.

http://dx.doi.org/10.21622/RESD.2016.02.2.096

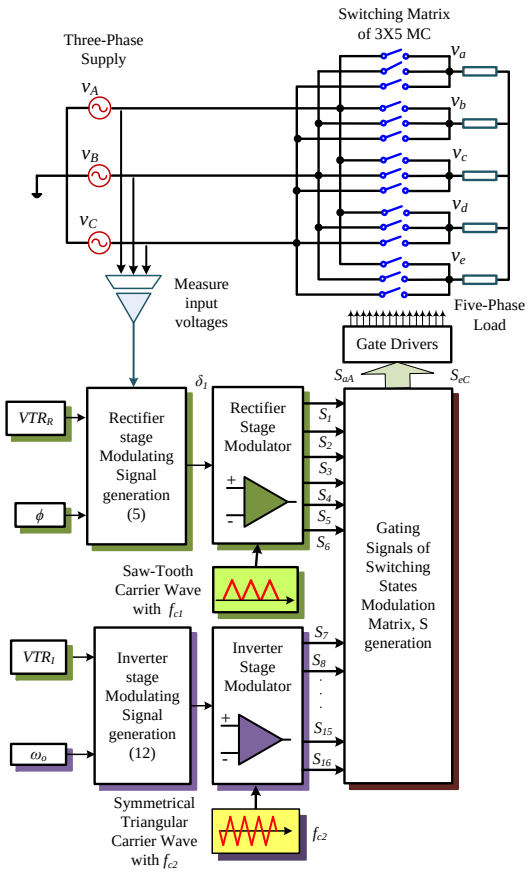

Fig .11. Layout of the implementation procedure of the proposed CBPWM technique

Finally, the generation of the overall gating signals of the 3×5 MC can be easily determined using (2) and (10). The final switching-state modulation matrix of the proposed 3×5 MC can be written as:

$$[S] = \begin{bmatrix} s_1s_7 + s_2s_8 & s_3s_7 + s_4s_8 & s_5s_7 + s_6s_8 \\ s_1s_9 + s_2s_{10} & s_3s_9 + s_4s_{10} & s_5s_9 + s_6s_{10} \\ s_1s_{11} + s_2s_{12} & s_3s_{11} + s_4s_{12} & s_5s_{11} + s_6s_{12} \\ s_1s_{13} + s_2s_{14} & s_3s_{13} + s_4s_{14} & s_5s_{13} + s_6s_{14} \\ s_1s_{15} + s_2s_{16} & s_3s_{15} + s_4s_{16} & s_5s_{15} + s_6s_{16} \end{bmatrix} \quad (16)$$

Fig. 12 illustrates the logic circuit that is used to generate the gating signals corresponding to phase-a of the 3×5 MC according to (20).

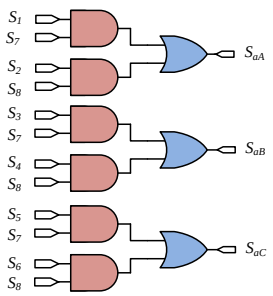

Fig .12. Generation of the gating signals of phase-a from the switching signals of the rectifier and inverter stages

VI. SIMULATION AND EXPERIMENTAL RESULTS

In order to verify the validity of the proposed modulation technique, a series of simulation and experimental results has been obtained in both linear and over-modulation operating modes. Firstly, to investigate the feasibility of the proposed modulation technique before compiling into a real-time system, the developed simulation models have been tested using Matlab/Simulink software. Then, a series of experimental tests were performed on the implemented 3×5 MC based on the dSPACE-DS1104 platform.

Fig. 13 shows a photograph of the complete experimental setup. In this figure, the host PC including the dSPACE controller, which is used to control and monitor the system variables by using the connector pins interface, is shown. Also, the power and interface circuits of the laboratory prototype of the proposed multi-phase MC are shown.

All measurements in this section are performed with a Tektronix MSO-2024B four-channel oscilloscope. The oscilloscope can also be logging the waveform data into the PC. These data can further be processed using MATLAB code in order to get the harmonic analysis of these waveforms.

In both the simulation and experimental processes, the 5-phase output terminals are connected to a series RL-load of 100 Ω and 0.25 H. In addition, A 100 V (peak), 50 Hz 3-phase voltage supply is applied to the 3-phase input terminals. In order to achieve a maximum available VTR of the 3×5 MC, the reference input current displacement angle has been adjusted to be equal zero.

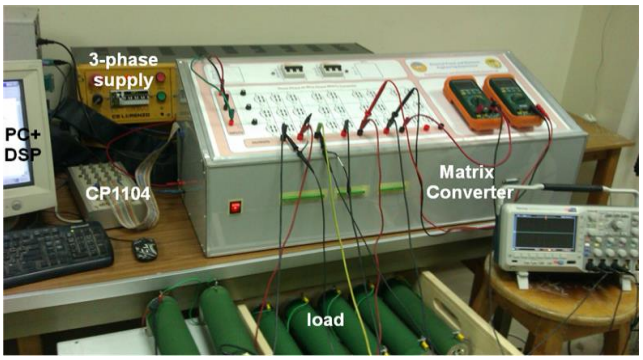

Fig .13. Photograph of the complete experimental set-up

On the other hand, the ratio of the carrier frequencies of both rectifier and inverter stages (f_{c1}/f_{c2}) is determined based on the Total Harmonic Distortion (THD) of the output current. Therefore, the operation of the 3×5 MC based on the proposed modulation technique is tested under a wide range of carrier-frequencies ratios and different frequencies of the output current. The THD of the output currents at different carrier-frequencies ratios (f_{c1}/f_{c2}) and different output-frequencies is shown in Fig. 14. The carrier-frequency range is changed from 1 kHz to 6 kHz.

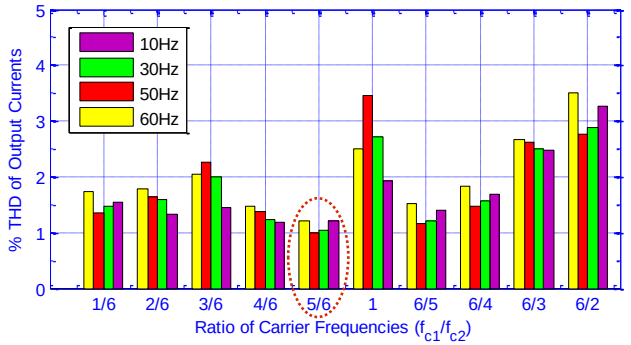

Fig .14. THD of output currents at different carrier-frequencies ratios and different output-frequencies

It can be noted from Fig. 14 that the THD of the output currents at different output-frequencies are in the acceptable limits (less than 5%) according to the specified standard of IEEE-519. In addition, it is observed that, in order to minimize the THD of the output currents, the ratio of the carrier frequencies should be selected as 5/6. Therefore, the simulation and experimental results, in both the linear and over-modulation modes, are obtained at carrier frequencies of the rectifier and inverter stages of 1.67 kHz and 2 kHz, respectively. In addition, the output frequency is set to 10Hz.

A. Modulation of Rectifier stage

The output line-line (adjacent and non-adjacent) and phase voltages generated by the 3×5 MC, in the linear modulation mode, are shown in Fig. 15 and Fig. 16, respectively. In order to achieve a maximum overall VTR of 0.7887 in the linear operating mode, both stages are operating with a maximum voltage transfer ratio in the linear operating mode (VTR_R = 1.5 and VTR_I = 0.5258).

Fig. 17 shows the FFT (harmonics spectrum) analysis of the phase-*a* output voltage. From which, it can be noted that the fundamental component of the output phase-voltage equals 78.8 percent of the input phase-voltage. In addition, dominant harmonic components around the switching frequency (harmonics order of 200) and its multiples can be easily observed.

Furthermore, the corresponding load-current waveforms are shown in Fig. 18. Due to the capability of the used oscilloscope, only 4-phase current waveforms are obtained in the experimental process. Balanced load currents with approximately sinusoidal waveform can be easily noted from Fig. 18. This is due to the load inductive-nature and the proposed modulation technique.

On the other hand, Fig. 19 shows the input-phase voltage and current waveforms of the 3×5 MC. It can be observed that the input current has a pulse width modulated waveform. Due to setting the input-current displacement angle to zero, it is found that the fundamental component of the input current is in-phase with the input voltage. Therefore, a unity input power-factor operation is obtained.

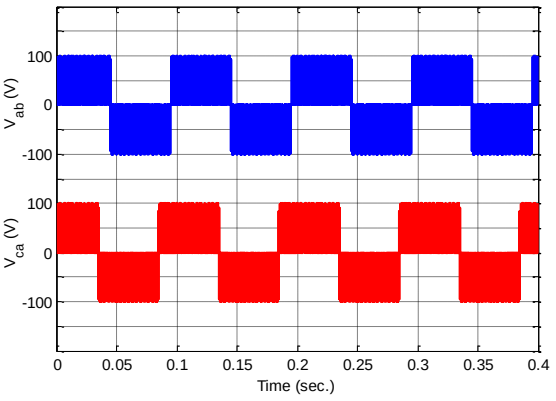

(a) Simulation

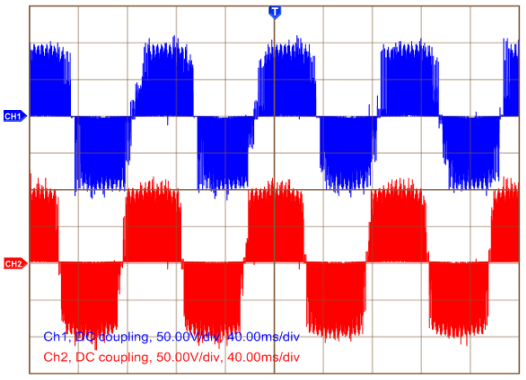

(b) Experimental (50 V/div.& 40 ms/div.)

Fig .15. Output adjacent and non-adjacent line-line voltage in the linear modulation operating mode at f_o=10 Hz

http://dx.doi.org/10.21622/RESD.2016.02.2.096

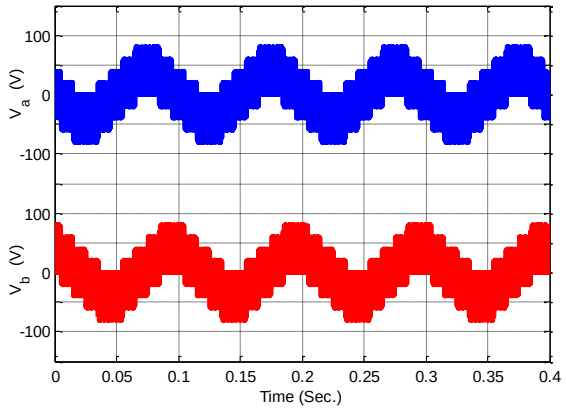

(a) Simulation

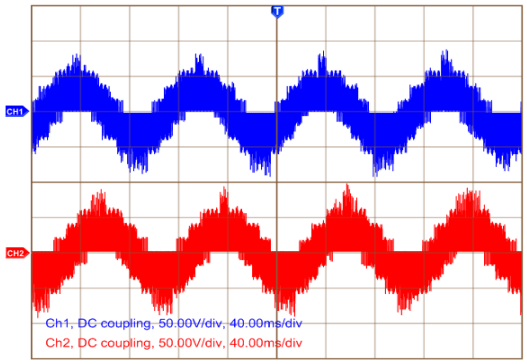

(b) Experimental (50 V/div.& 40 ms/div.)

Fig .16. Output phase voltage waveforms in the linear modulation operating mode at f_o=10 Hz

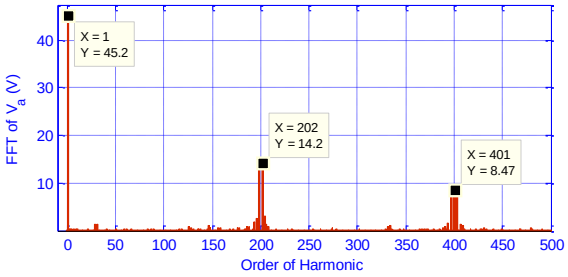

Fig .17. Harmonic spectrum analysis of phase-a of the output voltage in the linear operating mode at f_o=10 Hz

B. Over-modulation operating mode

In this operating mode, both rectifier and inverter stages are operating with a maximum voltage transfer ratio (VTR_R=1.654 and VTR_I = 0.636) at an output frequency of 10 Hz.

The generated output line-line (adjacent and non-adjacent) and phase voltages in over-modulation mode are shown in Fig. 20 and Fig. 21, respectively. In addition, the corresponding harmonics spectrum analysis of the phase-*a* output voltage is shown in Fig. 22. The obtained results in this operating mode show that the fundamental component of the output phase-voltage equals 105 percent of the input phase-voltage and therefore a maximum overall VTR is achieved.

Moreover, it can be observed that the output phase-voltage waveform contain a considerable amount of lower order harmonics as illustrated in Fig. 22. It can also be noted that the magnitude of each harmonic component equals the inverse of its order as a percentage of the fundamental component.

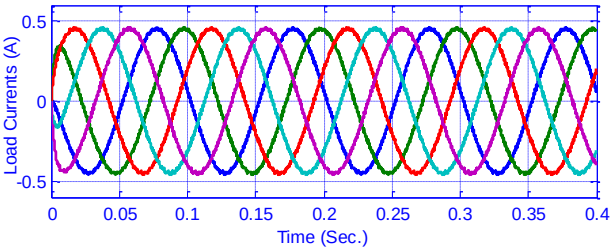

(a) Simulation

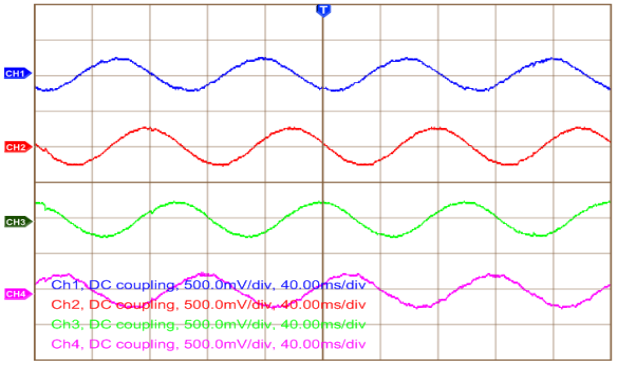

(b) Experimental (1 A/div.& 40 ms/div.)

Fig .18. Load-current waveforms in the linear modulation operating mode at f_o=10 Hz

On the other hand, Fig. 23 shows the load-current waveforms in the over-modulation operating mode. The discrepancy between these current waveforms and that shown in Fig. 18 is due to operating in over-modulation mode. Therefore, it can be concluded that, in the over-modulation operating mode, the load currents contain a considerable amount of lower order harmonics as can be observed form Fig. 23. Furthermore, the input-phase voltage and current waveforms in the over-modulation mode are shown in Fig. 24. A unity input power-factor operation can be easily observed due to setting the input-current displacement angle to zero.

A close agreement between the presented simulation and experimental results can easily be observed in both linear and over-modulation operating modes which verifies the effectiveness of the proposed modulation technique.

VII. COMPARISON BETWEEN THE PROPOSED CBPWM AND THE SVM TECHNIQUES FOR CONTROLLING 3×5 MC

In order to ensure the capability and effectiveness of the proposed modulation technique, a comparative study between the proposed CBPWM and the SVM techniques, given in [14], [15], for controlling the 3×5 MC is summarized in the following points:

- Unlike the SVM approach in [14], [15], the need for sector information for both input and output sides of the converter and the corresponding switching-tables are avoided in the CBPWM approach, thus highly simplifying the control of MCs, especially when the input or output phases are increased.

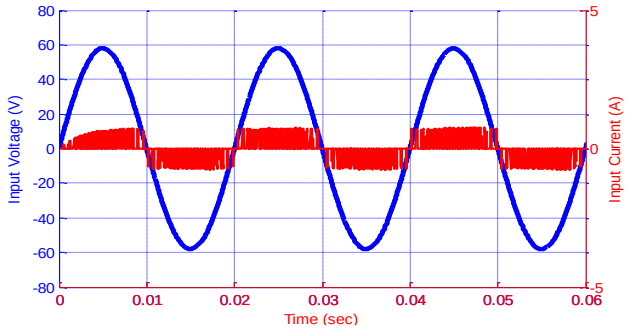

(a) Simulation

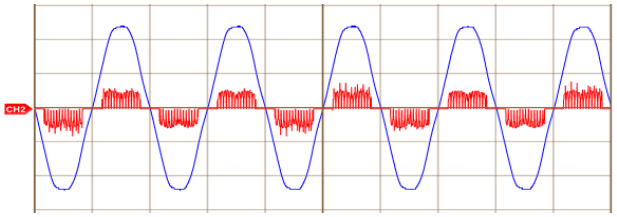

(b) Experimental (25 V/div., 1 A/div. & 40 ms/div.)

Fig .19. Input-phase voltage and current waveforms in the linear modulation operating mode.

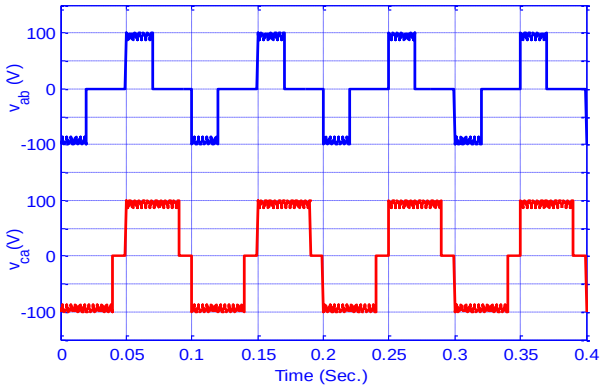

(a) Simulation

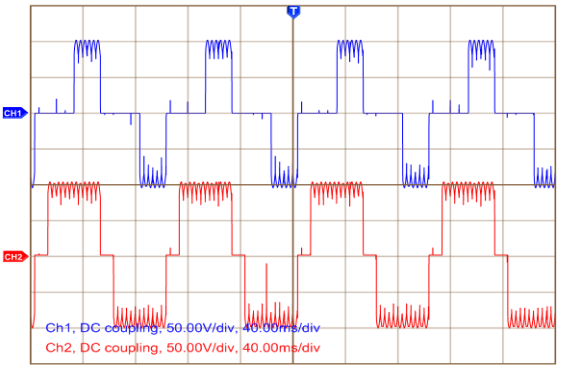

(b) Experimental (50 V/div.& 40 ms/div.)

Fig .20. Output adjacent and non-adjacent line-line voltage in over-modulation operating mode at f_o=10 Hz

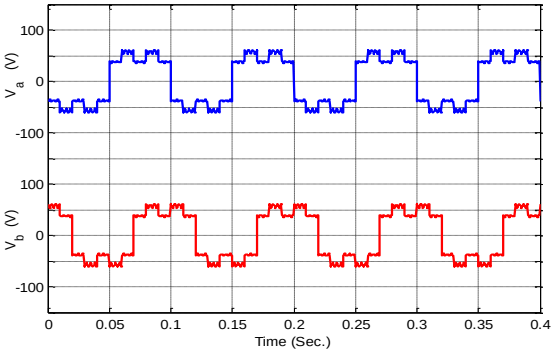

(a) Simulation

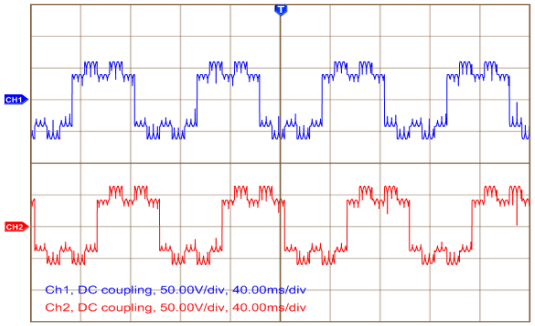

(b) Experimental (50 V/div.& 40 ms/div.)

Fig .21 Output phase-voltage waveforms in over-modulation operating mode at f_o=10 Hz

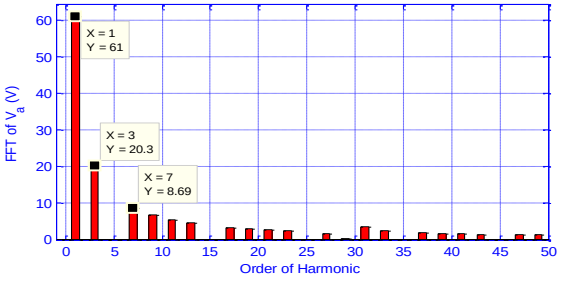

Fig .22 Harmonic spectrum analysis of phase-a of the output voltage in over-modulation operating mode at f_o=10 Hz

http://dx.doi.org/10.21622/RESD.2016.02.2.096

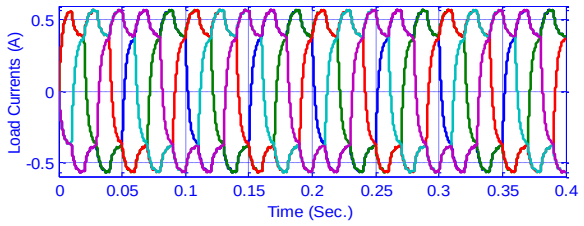

(a) Simulation

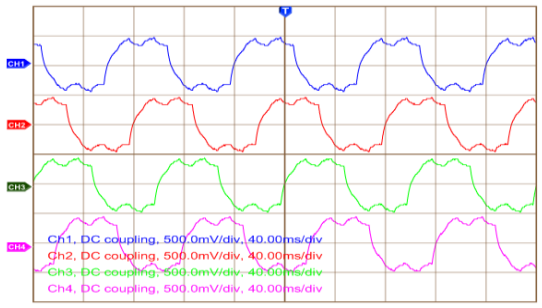

(b) Experimental (25 V/div., 1 A/div. & 40 ms/div.)

Fig .23. Load-currents-waveforms associated with over-modulation operating mode at f_o=10 Hz

- The maximum allowable VTR in the SVM approach in [14] and using scheme-II in [15] is 78.87%. The same value is obtained in the linear modulation mode of the CBPWM technique.

- In order to increase the VTR of the converter, both techniques push the converter to operate in the overmodulation region. The SVM approach in [15] increases the VTR to 92.3% using scheme-I, while the overmodulation-operating region in CBPWM is classified into three different modes (RSO, ISO and BSO). The maximum obtainable VTR of the converter is achieved using BSO mode to 105.2%.

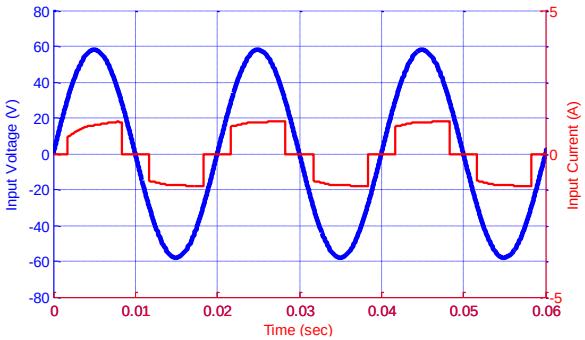

(a) Simulation

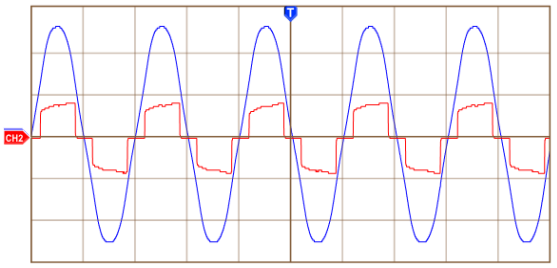

(b) Experimental (25 V/div., 1 A/div. & 40 ms/div.)

Fig .24. Input-phase voltage and current waveforms associated with the over-modulation operating mode

Fig. 25 shows the THD of the output voltage and current using both techniques for a wide frequency range. The output frequency is changed from 5 to 100 Hz, with an incremental step of 5 Hz. it can be observed that the THD for both output voltage and current in SVM is lower than CBPWM at all frequencies. Moreover, the output current THD in both techniques are below the IEEE standard requirements.

VIII. CONCLUSION

In this paper, a proposed CBPWM technique for a 3×5 MC has been presented. The proposed modulation technique has been based on the indirect configuration of the 3×5 MC, which assumes the converter as a virtual three-phase rectifier followed by a five-phase VSI. The proposed CBPWM technique has been applied for each stage independently including both linear and over-modulation operating modes. In order to verify the validity of the proposed modulation technique, a series of simulation and experimental results has been obtained in both modes of operation. It has been observed that, in order to minimize the THD of the output currents, the ratio of the carrier frequencies should be selected as 5/6. In addition, a maximum overall VTR of 0.7887 has been achieved in the linear operating mode when both stages are operating with a maximum voltage transfer ratio. Dominant harmonic components around the switching frequency and its multiples have also been observed. On the other hand, in the over-modulation operating mode, the fundamental component of the output phase-voltage has been found to be equal 105 percent of the input phase-voltage and therefore a maximum overall VTR has been also achieved. However, it has been observed that the output phase-voltages as well as the load currents obtained in this mode of operation have contained a considerable amount of lower order harmonics. A unity input power-factor operation has been achieved in both operating

modes due to setting the input-current displacement angle to zero. A close agreement between the presented simulation and experimental results in both linear and over-modulation operating modes has confirmed the effectiveness of the proposed modulation technique.

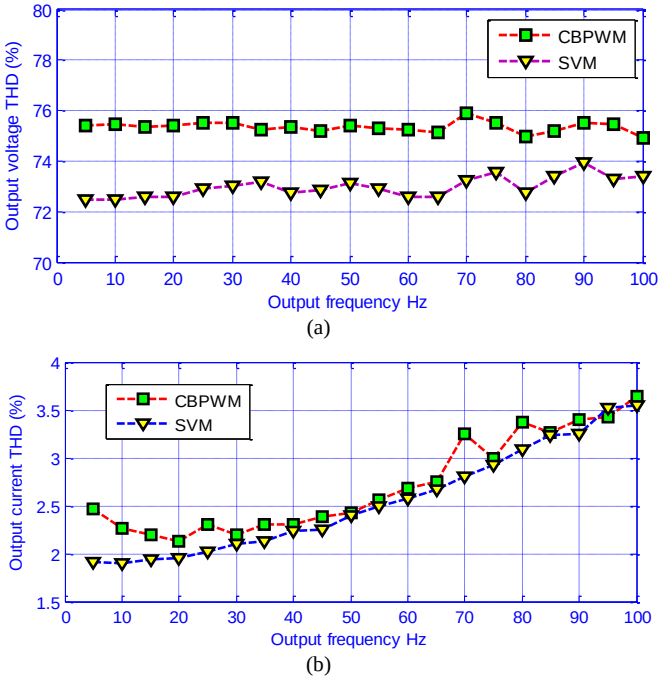

Fig .24. The THD for (a) Output voltage (b) Output current for the both CBPWM and SVM techniques

IX. BIOGRAPHY

Said M. Allam was born in Basyun, Egypt in 1977. He received the B. Sc., M.Sc. and Ph.D degrees in Electrical Power and Machines Engineering from Tanta University, Egypt in 2000, 2004 and 2009, respectively. He is currently an assistant professor at the Department of Electrical Power and Machines Engineering, Faculty of Engineering, Tanta University. His research interests are in Electrical Machines, Electrical Drives, Power Electronics and renewable energy.

Sherif M. Dabour received the B.Sc. degree from Zagazig University in 2002 and the M.Sc. and Ph.D. degrees in electrical power and machines engineering from Tanta University, Egypt, in 2012 and 2015 respectively. From 2003 to 2009, he was a certified trainer at the Technical and Vocational Training Corporation in Riyadh, KSA. Since 2009, he has joined the Faculty of Engineering, Tanta University, Egypt. Dr. Dabour is currently an assistant Professor with the Department of Electrical Power and Machines Engineering, Faculty of Engineering, Tanta University. His research interests are in the area of power electronics and electric drives.

Essam M. Rashad (S.M. 2002) was born in Shebin El-Kom, Egypt in 1960. He graduated from Faculty of Engineering, Menoufiya University, Egypt in 1983. Then he obtained his M.Sc. and Ph.D. degrees in Electrical Engineering from Alexandria University, Egypt in 1987 and 1992, respectively. He worked as an offshore maintenance engineer in Belayim Petroleum Company from 1985 to 1990. In 1992, he joined Faculty of Engineering, Tanta University, Egypt, where he is currently a Professor and Head of Electrical Power and Machines Engineering Department. His research interests include electrical machine analysis, electrical drives, power electronics and renewable energy.

REFERENCES

[1] L. Empringham, J. W. Kolar, J. Rodriguez,; P. W. Wheeler, J. C. Clare, , "Technological issues and industrial application of MCs: A Review," IEEE Trans. on Indus. Electro., vol.60, no.10, pp.4260-4271, 2013.

[2] J. Szczepanik, "Multiphase MC for power systems application," in Proc. of International Symposium in Power Electronics, Electrical Drives, Automation and Motion, Istanbul, pp.772-777, 2008.

[3] L. Rmili , S. Rahmani and K. Al-Haddad, “A review of indirect MC topologies," Journal of Renewable Energy and Sustainable Development (RESD), pp. 30-37, June 2015.

[4] L. Huber and D. Borojevic, “Space vector modulated three-phase to three-phase MC with input power factor correction,” IEEE Trans. Ind. Appl, vol. 31, no. 6, pp.1234-1246, 1995.

[5] S. M. Dabour, E. M. Rashad, "Analysis and implementation of space-vector-modulated three-phase matrix converter," Power Electronics, IET , vol.5, no.8, pp.1374-1378, 2012.

[6] T. D. Nguyen and L. Hong-Hee, "Generalized carrier-based PWM method for indirect matrix converters," in Proc. of Sustainable Energy Technologies (ICSET), 2012 IEEE Third International Conf., Kathmandu, pp.223-228, 2012.

[7] S. M. Dabour and E. M. Rashad, “A new continuous PWM strategy for three-phase direct MC using indirect equivalent topology’, in Proc. of IET International Conference on Power Electronics, Machines and Drives, PEMD-2014,

Manchester, UK, pp. 1-6, 2014.

[8] S. M. Ahmed, A. Iqbal, H. Abu-Rub, J. Rodriguez, C. A. Rojas, and M. Saleh, , "Simple carrier-cased PWM technique for a three-to-nine-phase direct AC–AC converter," IEEE Trans. Ind. Electro., vol.58, no.11, pp.5014-5023, 2011.

[9] M. Venturini, "A new sine wave in sine wave out, conversion technique which eliminates reactive elements," in Proc. of Powercon 7, pp. E3/1-E3/15, 1980.

[10] A. Alesina, M. Venturini, "Analysis and design of optimum-amplitude nine-switch direct AC-AC converters," IEEE Trans. Power Electronics, vol.4, no.1, pp.101-112, 1989.

[11] L. Hong-Hee , H. M. Nguyen, and C. Tae-Won, "New direct-SVM method for MC with main input power factor compensation" in Proc. of the 34th Annual Conference of Industrial Electronics, IECON 2008, Orlando, FL, pp. 1281-1286, 2008.

[12] H. M. Nguyen, L. Hong-Hee and C. Tae-Won, "An investigation on direct space vector modulation methods for matrix converter," in Proc. of IEEE 35th Annual Conference of Industrial Electronics, 2009, IECON '09, pp.4493-4498, 2009.

[13] E. M. Rashad, and S. M.Dabour, "A novel five-phase MC using space vector modulation control algorithm," Engineering Research Journal, vol. 34, no.4, pp.321-328, 2011.

[14] A. Iqbal, S. M. Ahmed and H. Abu-Rub, "Space vector PWM technique for a three-to-five-phase MC," IEEE Trans. on Ind. App., vol.48, no.2, pp.697-707, 2012.

[15] S. M. Dabour, A. W. Hassan and E. M. Rashad, "Analysis and implementation of space vector modulated five-phase matrix converter," International Journal of Electrical Power & Energy Systems, vol 63, pp. 740–746, 2014.

[16] T. D. Nguyen and; L. Hong-Hee, "Carrier-based PWM technique for three-to-five phase indirect matrix converters," in Proc. of 37th Annual Conference on IEEE Industrial Electronics Society, Melbourne, VIC, pp.3662-3667, 2011.

[17] M. Saleh, A. Iqbal, S. M. Ahmed, and A. Kalam, "Matrix converter based five-phase series-connected two-motor drive system," in Proc. of Universities Power Engineering 22nd Conference (AUPEC 2012), Australia, pp.1-6, 26-29 2012.

[18] M. Saleh, A. Iqbal, S. M. Ahmed, H. Abu Rub, and A. Kalam, , "Carrier based PWM technique for a three-to-six phase MC for supplying six-phase two-motor drives," in Proc. of 37th Annual Conference on IEEE Industrial Electronics Society, Melbourne, VIC, pp.3470-3475, 2011.

[19] W. Haibing, R. Zhao,, F. Cheng and H. Yang, "Six-phase induction machine driven by the matrix converter," in Proc. of Inter. Conf. in Electrical Machines and Systems (ICEMS), 2011, Beijing, pp.1-5, 2011.

[20] S. K. M. Ahmed, A.Iqbal, H. Abu-Rub, and M. R. Khan, , "Carrier based PWM technique for a novel three-to-seven phase matrix converter," in Proc. International Conf. in Electrical Machines (ICEM 2010), Rome, pp.1-6, 2010.

[21] S. K. M. Ahmed, A. Iqbal,; H. Abu-Rub, "Generalized duty-ratio-based pulse width modulation technique for a three-to-k phase MC," IEEE Trans. on Indus. Electro., vol.58, no.9, pp.3925-3937, 2011.

[22] S. M. Ahmed, H. Abu-Rub, Z. Salam, and A.Kouzou, , "Space vector PWM technique for a novel three-to-seven phase matrix converter," in IEEE 39th Annual Conference of Industrial Electronics Society, IECON 2013, Vienna, pp.4949-4954, 2013.

[23] K. Rahman,; A. Iqbal,; A. A. Abduallah,; R. Al-Ammari and H. Abu-Rub, "Space vector pulse width modulation scheme for three to seven phase direct matrix converter," Annual IEEE Applied Power Electronics Conference and Exposition, (APEC 2014), Fort Worth, TX, pp.595-601, 2014.

[24] S. M. Dabour, S. M. Allam, and E. M. Rashad, "Space vector PWM technique for three- to seven-phase matrix converter," in Proc. of 16th International Middle East Power System Conf.,

MEPCON 2014, Egypt, pp.1-6, 2014.

[25] K. K. Mohapatra,, P. Jose, A. Drolia, G. Aggarwal and S. Thuta, “A novel carrier-based PWM scheme for matrix converters that is easy to implement," in Proc. of the 36th IEEE Power Electronics Specialists Conference, 2005 (PESC '05), Recife, pp.2410-2414, 2005.

[26] S. Thuta, K. K. Mohapatra,and N. Mohan, , "Matrix converter over-modulation using carrier-based control: Maximizing the voltage transfer ratio," in Proc. Of IEEE Power Electronics Specialists Conference, 2008 (PESC 2008), Rhodes, pp.1727-1733, 2008.

[27] S. M. Dabour, S. M. Allam and E. M. Rashad, “A simple CB-PWM technique for Ffive-phase MCs, including overmodulation mode,” in Proc. of the 8th IEEE GCC Conference and Exhibition (GCCCE), Muscat, pp.1-6, 2015.

[28] M. I. Masoud, S. M. Dabour, A. E. W. Hassan and E. M. Rashad, "Control of five-phase induction motor under open-circuit phase fault fed by fault tolerant VSI," in Proc. of the IEEE 10th Inter. Symposium on Diagnostics for Electrical Machines, Power Electronics and Drives (SDEMPED), Guarda, pp. 327-332, 2015.

[29] D. Dujic, M. Jones, and E. Levi, “Continuous carrier-based vs. space vector PWM for five-phase VSI,” in Proc. of Inter. Conf. on Computer as a Tool EUROCON, 2007, Warsaw, 2007,pp.1772-1779, 2007.

[30] M. I. Masoud and S. M. Dabour, “Investigation of five-phase induction motor drive under faulty inverter conditions," in Proc. of IEEE Inter. Conf. on Industrial Technology (ICIT2015) , pp. 1-6, 2015.

[31] A. Iqbal, S. Moinuddin, and M.R. Khan, "Space vector operating model of a five-phase voltage source inverter," in Proc. of IEEE Inter. Conf. on Industrial Technology, (ICIT2006), Mumbai, pp.488-493, 2006.

[32] A. Iqbal, E. Levi, M. Jones, and S. N. Vukosavic, “Generalised sinusoidal PWM with harmonic inject ion for multi-phase VSIs,” in Proc. of the 37th IEEE Power Electronics Specialists Conference, 2006. PESC '06, Jeju, pp.1-7, 2006.

[33] S. K. Gupta, M. A. Khan, A. Iqbal, and Z. Husain, “Comparative analysis of pulse width modulation schemes for five phase voltage source inverter,” in Proc. of Engineering and Systems (SCES), 2012 Students’ Conf., Allahabad, Uttar Pradesh, pp.1-6, 2012.